TENSILE BEHAVIORS AND FRACTURE CHARACTERISTICS OF LAMINATED Ti6Al4V-TiBw/Ti6Al4V COMPOSITES ALONG TRANSVERSE AND LONGITUDINAL DIRECTIONS

B.X. Liu, L.J. Huang*, B. Wang, L. Geng

School of Materials Science and Engineering, Harbin Institute of Technology, P.O. Box433, Harbin 150001, China
**huanglujun@hit.edu.cn.*

Keywords: laminated composites, mechanical property, strengthening effect, fracture elongation.

Abstract
A novel laminated composites containing Ti6Al4V layers and TiB whisker reinforced Ti6Al4V composites (TiBw/Ti6Al4V) layers was successfully fabricated by reaction hot pressing. The in-situ reacted TiB whiskers and their network distribution structures obviously change the Ti6Al4V matrix from coarse widmanstatte microstructure into lath-like and near equiaxed microstructure. The longitudinal tensile behaviors show that the elongation and the ultimate strength of laminated composites can be increased to 12.5% and 1120MPa, indicating the strengthening effect of unique distribution structures of in-situ TiB whiskers. Moreover, it is interesting to note that transverse tensile behaviors show that the elongation and the ultimate strength of laminated composites can gain 7.8% and 1020MPa, which are seriously deviate the series laws using lamination theory.

1. Introduction

The applications of discontinuously reinforced titanium matrix composites (DRTMCs) have attracted more and more attention in automobile, aerospace and armor industries over conventional Ti and its alloys due to their high room temperature and high temperature strength [1-4]. However, due to the incorporation of fibrous, whisker and particulate reinforcements by both ex-situ and in situ methods, titanium matrix composites (TMCs) usually exhibit low ductility and toughness in comparison with monolithic titanium and titanium alloys [5], which greatly limits their practical application. Fang et. at proposed an idea that the mechanical properties of copper can be enhanced by tailoring the distribution of grain to form novel multi-scale structures far beyond the homogeneous grain structure [6]. Recently, a novel network distribution of reinforcement resulted in a significant strengthening effect and high fracture toughness of TiBw/Ti composites in which the TiB whisker-rich boundary region imparts the superior strengthening effect and a relatively large TiB whisker-lean region contributes the ductility of the composites [7, 8]. Meanwhile, the design of laminated structures is becoming a prevailing idea in developing high fracture toughness of titanium matrix composites [9].

Laminated composites have been extensively studied for a number of potential applications: structural components, aerospace sector, automobile and armor. Typical laminated composites such as ceramic-ceramic, metal-ceramic, metal-metal and metal-ceramic-intermetallic systems have shown desirable properties [10]. These systems allow for the possibility of combining the good ductility and toughness of the metal matrix with the high strength of reinforcements. There are several processing techniques, such as adhesion bonding, chemical deposition, diffusion bonding, hot accumulative rolling, flake powder metallurgy and reactive sintering used to fabricate these laminated systems [11].

Recently, some studies have been performed in the fracture toughness and fatigue properties of functionally graded TiBw/Ti composites. These materials always behave in a brittle manner under bending stress or shearing force due to the high volume fraction of TiB phase [12-14]. In contrast to the vast number of studies conducted toward understanding the crack propagation behavior in laminated composites with high volume fraction of reinforcements, ductile tensile behavior with a view to enhancing ductility has rarely been investigated in laminated composites with low volume fractions of reinforcements.

In this study, Ti6Al4V-TiBw/Ti6Al4V multi-layered composites were prepared with Ti6Al4V and TiB_2 powders via reaction hot pressing. The microstructure and mechanical properties of the composites were investigated; the fracture failure process of the composites under tensile loading was consecutively observed and the related failure mechanism was discussed based on the experimental observation.

2. Experimental procedures

In this paper, a novel laminated Ti6Al4V-TiBw/Ti6Al4V composite was successfully fabricated by reaction hot pressing based on design concepts of Yin, Huang [11] and Lu [6]. Two-scale laminated composites were presented in the novel composites: layer structure in macro-scale and three-dimensional (3D) network distribution structure of TiB whiskers in meso-scale. The fabrication process is shown in Fig. 1 as follows: (1) Ball milling with the speed of 200r/min and time of 8h, the fine TiB_2 powders (Fig. 1b)) will be homogeneously adhered to the large Ti6Al4V sphere powders (Fig. 1a)). (2) The blended powders (Fig. 1c)) and pure Ti6Al4V powders were quantitatively stacked layer by layer. (3) Reaction hot pressing in vacuum (10^{-2}Pa) at 1200^{o}C under a pressure of 25MPa for 40min. TiB phase is in situ synthesized according to the following reaction:

$$Ti + TiB_2 \rightarrow 2TiB \quad (1)$$

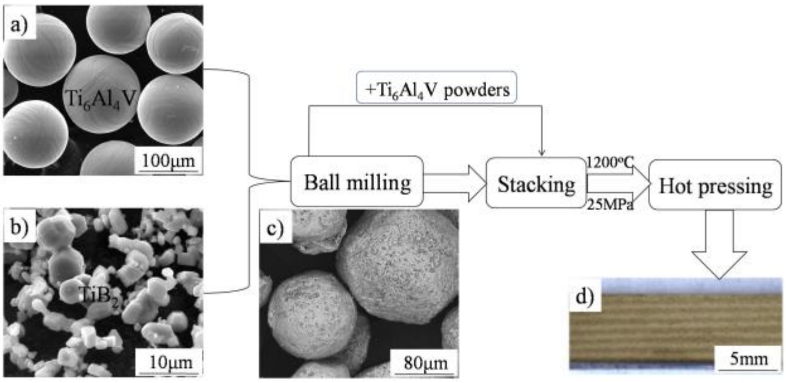

Fig. 1. The fabrication process diagram of the laminated Ti6Al4V-TiBw/Ti6Al4V composites. a) raw titanium powders; b) TiB_2 powders; c) mixture powders; d) laminated Ti6Al4V-TiBw/Ti6Al4V composites.

Finally, the thickness of two different layers is also 0.4mm, which can be shown in Fig. 1d). It is well known that the TiB phase is thermodynamically more stable than TiB_2 phase with excess Ti. Based on the reaction (1), the laminated Ti6Al4V-TiBw/Ti6Al4V composites containing Ti layer and titanium matrix composite layer with network reinforcement distribution were fabricated. The TiBw volume fraction in the TiBw/Ti6Al4V composite layer is 3 vol. %. Therefore, the average volume fraction of TiBw in the laminated composites is about 1.5 vol. %.

Microstructural examination was performed by optical microscopy (OM) and scanning electron microscopy (SEM, Hitachi S-4700) with the sample surfaces etched by 5%HF+15%HNO_3+85%H_2O solution. Phase analysis of laminated Ti-TiBw/Ti composites was carried out by X-ray diffractometer (XRD). Tensile tests were carried out using an Instron-5569 universal testing machine at a constant crosshead speed of 2mm/min. Tensile dog bone samples have dimensions of 18mm×5.6mm×2mm and a total of five samples were tested for each material.

3. Results and discussions

3.1. XRD Analysis

XRD was utilized on laminated Ti6Al4V-TiBw/Ti6Al4V composites after being pressed are shown in Fig. 2. The laminated Ti6Al4V-TiBw/Ti6Al4V composites contains α-Ti, β-Ti and TiB phase peaks, there are no peaks of TiB_2 presented in the spectra, indicating that chemical reaction (1) was completed during the reaction hot pressing process and only TiB phase was synthesized as expected.

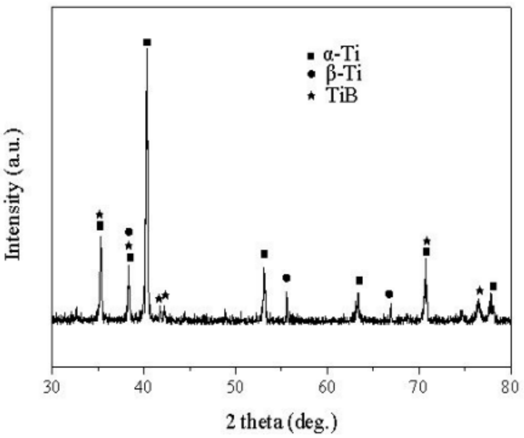

Fig. 2. XRD patterns of laminated Ti-TiBw/Ti composites.

3.2. Microstructure characteristics

Fig. 3 shows the SEM micrographs of the laminated Ti6Al4V-TiBw/Ti6Al4V composites fabricated at the temperature of 1200°C. Although distribution and thickness of layers are almost smooth and uniform in macro scale, there are a few single blended powders scattered in pure Ti6Al4V alloy layers as shown in Fig. 3a), it can be seen from the cross section of the laminated composites that wavy layered structure without porosity and crack has formed, which indicates that a well-bonded composite structure can be achieved by sintering process as shown in Fig. 3b). The thicknesses of the bright TiBw/Ti6Al4V composite layer and dark Ti6Al4V layer are about 400μm. It can be clearly seen from Fig. 3c) that TiB whiskers distribute around Ti particles, and form three-dimensional (3D) irregular and flattened networks with a diameter about 80-120μm equal to the size of raw Ti powders, this anistotropic network distribution of TiB whiskers is attributed to the high pressure and the long holding time during the hot pressing. The TiB whiskers are tightly fixed to the Ti particles and no micro defects appeared due to good wetting and clean reaction interface between Ti and TiB whisker.

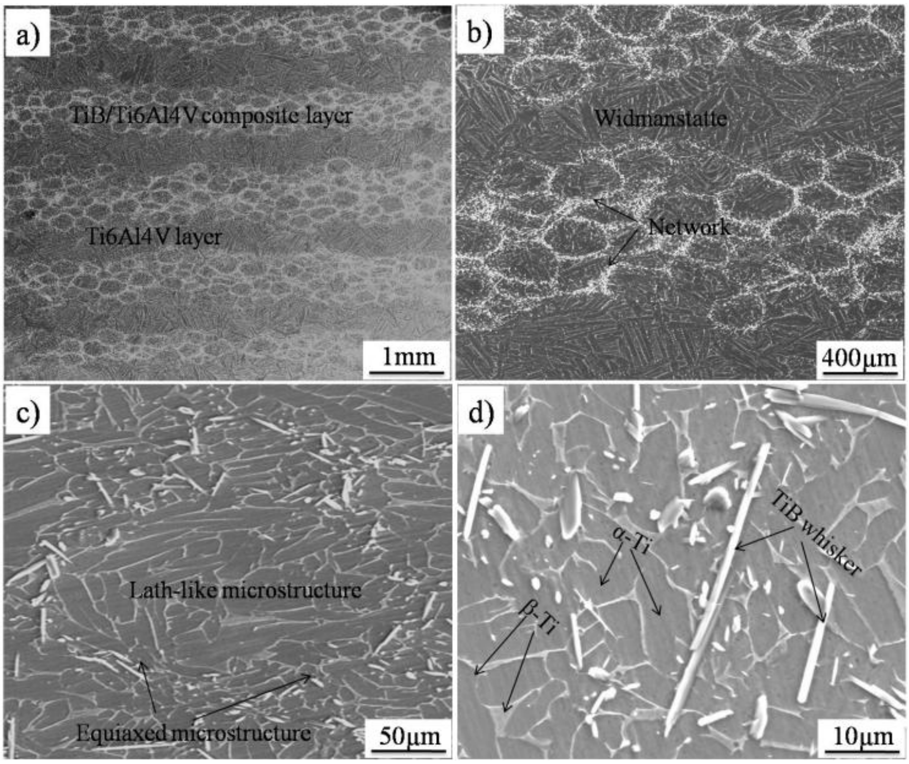

Fig. 3. SEM micrographs of laminated Ti-TiBw/Ti composites. a) low magnification; b) high magnification; c) TiBw/Ti composite layer; d) TiBw rich zone.

Figs. 3a) and 3b) show the matrix microstructure of two different layers. In the Ti6Al4V layer, it is to be found a typical coarse widmanstatte structure of (α/β) titanium alloys where individual α-laths are separated by a thin layer of retained prior β phase. However, the prior coarse equiaxed β phase is not distinguished due to the inhibiting effect of TiBw/Ti6Al4V composite layer. Fig. 3c) shows the network distribution of TiB whiskers in the TiBw/Ti6Al4V composite layer, it is interesting to note that many fine equiaxed α phases appear in the immediate zone of TiB whiskers but coarse lath-like α phases formed further away from TiB whiskers or inner of network, which is attributed to isotropic tensile stress generated by phase transition from β phase to α phase. Fig. 3d) shows the morphology of TiB phase. A large amount of needle shape TiB whiskers with high aspect ratio were formed around the raw Ti particles, which plays an important role in strengthening Ti matrix due to shear-lag model, grain refinement and dislocation proliferation mechanism.

3.3. Tensile behavior

The room-temperature engineering stress-strain curves of the laminated Ti6Al4V-TiBw/Ti6Al4V composites with longitudinal and transverse directions are shown in Fig. 4. It can be seen that the laminated Ti6Al4V-TiBw/Ti6Al4V composites with longitudinal direction exhibit an ultra-high plastic deformation capacity. Its yield strength reaches 872MPa, which is similar with that (870MPa) of laminated Ti6Al4V-TiBw/Ti6Al4V composites with transverse direction. However, the ultimate strength of laminated Ti6Al4V-TiBw/Ti6Al4V composites with longitudinal direction reaches 1120MPa, higher than that (1020MPa) of laminated composites with transverse tensile direction. This phenomenon may be attributed to the sufficient dislocation strengthening effect during the superior plastic deformation stage. The elongation of the laminated Ti6Al4V-TiBw/Ti6Al4V composites with longitudinal direction, approximating to 12.5%, is higher than that (7.5%) of laminated Ti6Al4V-TiBw/Ti6Al4V composites with transverse direction.

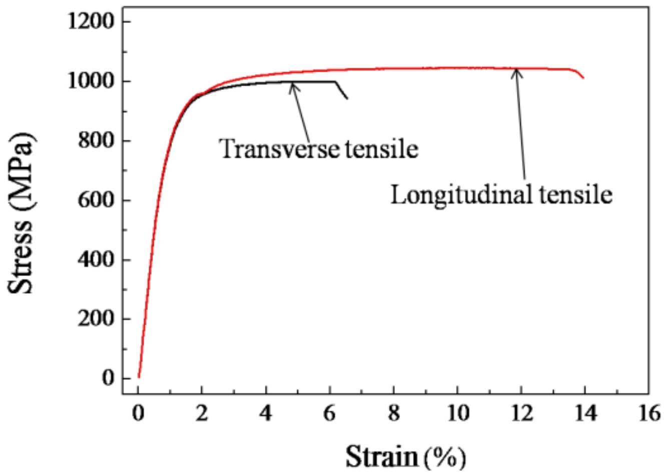

Fig. 4. The tensile stress- strain curves of laminated Ti6Al4V-TiBw/Ti6Al4V composites with longitudinal and transverse direction.

The SEM profile surface and crack propagation paths of the laminated Ti6Al4V-TiBw/Ti6Al4V composites with longitudinal direction are showed in Fig. 5. It can be clearly seen from the fractographs that the overall fracture surface is very rough indicating tortuous crack propagation paths. The Ti6Al4V layer reveals shear fracture propagating along 45 degree with the tensile direction, and the crack in the TiBw/Ti6Al4V composite layer propagates along the network boundary of in situ reacted TiB whiskers as shown in Fig. 5a). The typical characteristics of large scale plastic deformation are presented in the Ti6Al4V layer, such as shear bands and diffuse necking as shown in Fig. 5a) and Fig. 5b). Obviously, the widmanstatte structure becomes distorted and reveal anisotropy deformation manner: the width of widmanstatte structure is increased in the zone marked in f, whereas widmanstatte structure is elongated in the zone marked in g, as shown in Fig. 5b). Fig 5c) shows the crack in the TiBw/Ti6Al4V composites propagates along the network boundary with high volume fraction of TiB whiskers, indicating the network structure can play effectively role in strengthening Ti matrix. Meanwhile, some cracks are presented in the boundary of single blended powders scattered in the Ti6Al4V layer, which is attributed to the fractured and multi-fractured TiB whiskers as shown in Fig. 5d). Fig. 5e) shows the propagating manners of shear bands, some shear bands in the α phase pass through the thin β phase in the zone marked in h, whereas many shear bands in the α phase are inhibited by thick β phase in the zone marked in i.

The tortuous fracture morphologies of laminated Ti6Al4V-TiBw/Ti6Al4V are shown in Fig. 6. Obviously, the fracture surface of the Ti layer is composed of many dimples (Figs. 6a) and 6b)). It is confirmed that the Ti6Al4V layer underwent a large plastic deformation before failure occurred. Higher elongation-to-failure in Ti6Al4V layer can be correlated with the presence of fine and well-developed dimples as compared to quasi-cleavage fracture morphology in the TiBw/Ti6Al4V composites layer. Some coarse and deep dimples can be obtained by interconnecting and coalescence among many small dimples due to slip force in Ti6Al4V layer. It confirms that the Ti layer can bear large strain of the laminated Ti6Al4V-TiBw/Ti6Al4V composites during the tensile deformation.

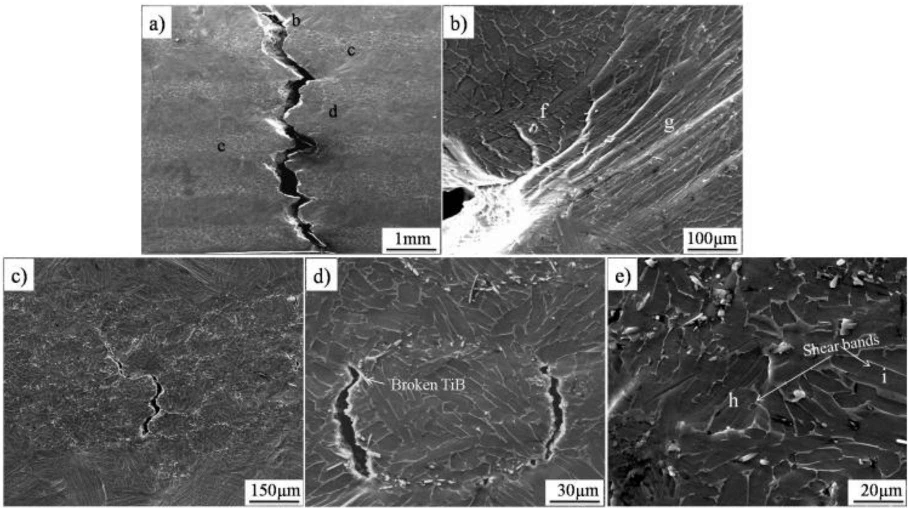

Fig. 5. The profile fracture surface of the laminated Ti6Al4V-TiBw/Ti6Al4V composites. a) low magnification; b) pure Ti6Al4V layer; c) TiBw/Ti6Al4V composite layer; d) fracture of single blended powders; e) propagating manners of shear bands.

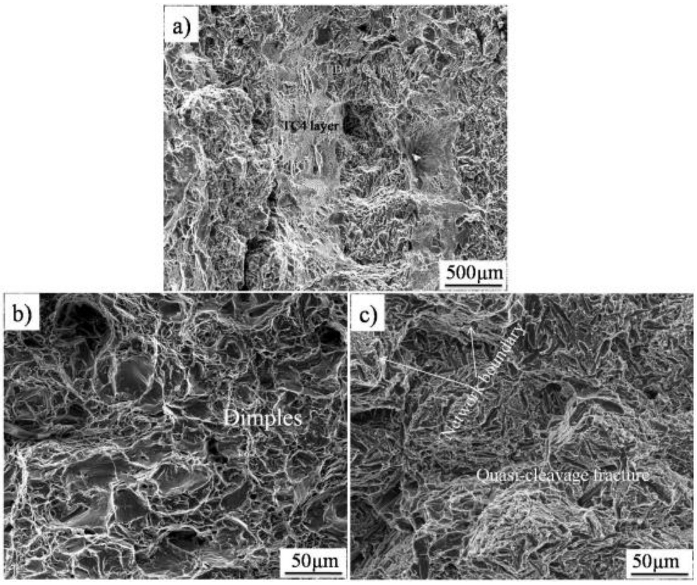

Fig. 6. The fractographs of the laminated Ti6Al4V-TiBw/Ti6Al4V composites. a) overall fracture surface; b) pure Ti6Al4V layer; c) TiBw/Ti6Al4V composite layer.

Compared to fine and well-developed dimples in the Ti6Al4V layer, the TiBw/Ti6Al4V composite layer reveals quasi-cleavage fracture morphologies including regions of many tearing ridge lines and flat "featureless" regions. It is found that many tearing ridge lines emerge at the TiB whiskers rich network zone, which indicates that the continuous matrix among the needle TiB whiskers can effectively play a toughening role. There is no evidence of large Ti6Al4V matrix rupture on the fracture surface and cracks always propagate along network distribution of TiB whiskers (Fig. 6c)). Besides, no TiB whiskers are pulled out, which is attributed to the strong interface cohesion between TiBw and Ti6Al4V matrix.

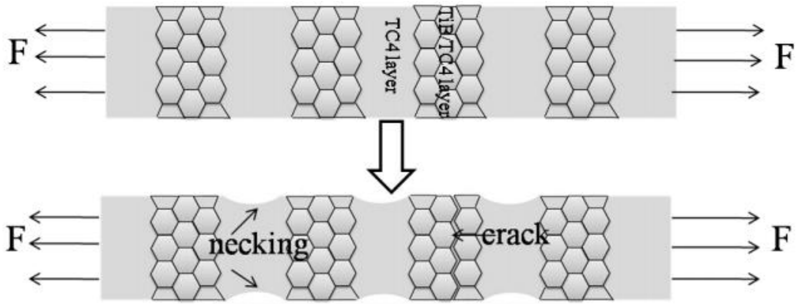

Fig. 7. Schematic diagrams representing the laminated Ti6Al4V-TiBw/Ti6Al4V composites failure mechanism.

The microstructure evolution and fracture mechanisms of laminated Ti-TiBw/Ti composites with longitudinal tensile direction have been reported in the previous work [15], and the crack initiation of laminated Ti6Al4V-TiB/Ti6Al4V composites is presented in the TiBw/Ti6Al4V composite layer, which always propagates along the network distribution of TiB whiskers. Fig. 7 shows the schematic diagram of the laminated Ti6Al4V-TiBw/Ti6Al4V composites failure mechanism with transverse tensile direction. The pure Ti6Al4V layer with low strength and low strain hardening rate affords high strain and TiBw/Ti6Al4V composite layer affords low strain during transverse tensile process, then there are two typical stress concentration presented in the Ti6Al4V layer and TiBw/Ti6Al4V composite layer: pure Ti6Al4V layer reveal many diffuse necking and TiBw/Ti6Al4V composite layer reveal many secondary cracks. The fracture failure will be occurred at one of states of $\varepsilon_{\mathrm{Ti6Al4V}} \geq \delta_{\mathrm{Ti6Al4V}}$ and $\varepsilon_{composite} \geq \delta_{composite}$, where ε is the tensile strain and δ is the tensile fracture elongation. Therefore, the fracture mainly formed in the TiBw/Ti6Al4V composite layer is attributed to that $\varepsilon_{composite}$ firstly reaches to $\delta_{composite}$.

4. Conclusions

(1) The novel laminated Ti6Al4V-TiBw/Ti6Al4V composites with wavy interfaces were successfully fabricated by reaction hot pressing. There are a few single blended powders scattered in pure Ti6Al4V alloy layers. The phase identification shows the in-situ reaction between Ti and TiB_2 was completed.

(2) In situ TiB whiskers obviously refine the matrix microstructure of laminated composite. In the Ti6Al4V layer, typical coarse widmanstatte structure of (α/β) titanium alloys is formed where individual α-laths are separated by a thin layer of retained prior β phase. In the TiBw/Ti6Al4V composite layer, many fine equiaxed α phases appear in the immediate zone of TiB whiskers but coarse lath-like α phases is formed further away from TiB whiskers or inner of network.

(3) The laminated composites with longitudinal direction exhibit a higher combination of tensile strength and ductility than the laminated composites with transverse direction. The fracture failure of laminated Ti6Al4V-TiB/Ti6Al4V composites with transverse tensile testing is presented in the TiBw/Ti6Al4V composite layer, which is attributed to that $\varepsilon_{composite}$ firstly reaches to $\delta_{composite}$.

Acknowledgements

This work is financially supported by the National Natural Science Foundation of China (NSFC) under Grant Nos. 51101042, 51271064 and 51228102, the High Technology Research and Development Program of China (863) under Grant No. 2013AA030902, the 5th-class Special Foundation (2012T50327) from the China Postdoctoral Science Foundation.

References

[1] M. Cariola. A high-potential sector: Titanium metal oligopolistic policies and technological constraints as main limits to its development. Resources Policy, 25: 151-159, 1999.

[2] L.G. Zhen, L.R. Ze. Non-aerospace application of Ti materials with a great many social and economic benefits in China. Mat. Sci. Eng. A, 280: 25-29, 2000.

[3] S.C. Tjong, Z.Y. Ma. Microstructural and mechanical characteristics of in situ metal matrix composites. Mat. Sci. Eng. R, 29: 49-113, 2000.

[4] K.S. Ravichandran, K.B. Panda, and S.S. Sahay. TiBw reinforced Ti composites Processing, properties, application prospects, and research needs. JOM, 56: 42-48, 2004.

[5] T.S. Srivatsan, W.O. Soboyejo, R.J. Lederich. The cyclic fatigue and fracture behavior of a titanium alloy metal matrix composite. Eng. Fract. Mech, 52: 467-491, 1995.

[6] Fang TH, Li WL, Tao NR, Lu K. Revealing extraordinary intrinsic tensile plasticity in gradient nano-grained copper. Science, 331: 1587-1590, 2011.

[7] H.X. Peng. A review of “Consolidation effects on tensile properties of an elemental Al matrix composite”. Mater. Sci. Eng. A, 386: 194–204, 2004.

[8] L.J. Huang, L. Geng, and H.X. Peng. In situ (TiBw+TiCp)/Ti6Al4V composites with a network reinforcement distribution. Mat. Sci. Eng. A, 527: 6723-6727, 2010.

[9] K.B. Panda, K.S. Ravichandran. Tianium-titanium boride (Ti-TiB) functionally graded materials through reaction sintering: synthesis, microstructure, and properties. Metall. Mater. Trans. A, 34: 1993-2003, 2002.

[10] S. Ohsaki, S. Kato, N. Tsuji. Bulk mechanical alloying of Cu-Ag and Cu/Zr two-phase microstructure by accumulative roll-bonding process. Acta Mater, 55: 2885-2895, 2007.

[11] L. Jiang, Z.Q. Li, G.L. Fan and D. Zhang. A flake powder metallurgy approach to Al_2O_3/Al biomimetic nanolaminated composites with enhanced ductility. Scripta Mater, 65: 412-415, 2011.

[12] S.S. Sahay, K.S. Ravichandran, R. Atri. Evolution of microstructure and phases in in situ processed Ti-TiB composites containing high volume fractions of TiB whiskers. J. Mater. Res, 14: 4214-4223, 1999.

[13] J. Ma, G.E.B. Tan, Z.M. He. Fabrication and Characterization of Ti-TiB_2 Functionally Graded Material System. Metall. Mater. Trans. A, 33: 681-685, 2002.

[14] A. Kidane, A. Shukla. Quasi-static and dynamic fracture initiation toughness of Ti/TiB layered functionally graded material under thermo-mechanical loading. Eng. Fract. Mech, 77: 479-491, 2010.

[15] B.X. Liu, L.J. Huang, L. Geng, B. Kaveendran, B. Wang, X.Q. Song, X.P. Cui. Gradient grain distribution and enhanced properties of novel laminated Ti-TiBw/Ti composites by reaction hot-pressing. Mater. Sci. Eng. A, 595: 257-265, 2014.